ELEVENTH EUROPEAN ROTORCRAFT FORUM

Paper No. 72

FINITE STATE MODELLING OF UNSTEADY AERODYNAMICS AND ITS APPLICATION TO A ROTOR DYNAMIC PROBLEM

P.P. Friedmann and C. Venkatesan
Mechanical, Aerospace and Nuclear Engineering Department
University of California at Los Angeles
Los Angeles, California 90024, U.S.A.

September 10-13, 1985

London, England.

THE CITY UNIVERSITY, LONDON, EC1V OHB, ENGLAND.

FINITE STATE MODELLING OF UNSTEADY AERODYNAMICS AND ITS APPLICATION TO A ROTOR DYNAMIC PROBLEM*

P.P. Friedmann† and C. Venkatesan††
Mechanical, Aerospace and Nuclear Engineering Department
University of California at Los Angeles
Los Angeles, California 90024, U.S.A.

ABSTRACT

The paper presents a method for formulating finite state unsteady aerodynamic models in the time domain from frequency domain unsteady aerodynamics. The method is based on recognizing that the lift deficiency function represents an aerodynamic transfer function and utilizes the Bode plot technique, used in control systems engineering, to construct approximation to the lift deficiency function. Indicial response functions for both fixed wing and rotary wing applications are obtained, using these finite state unsteady aerodynamic models. It is shown that the rotary wing indicial response function is oscillatory and thus it is fundamentally different when compared to the fixed wing indicial response function which is nonoscillatory. Certain aspects of the finite state aerodynamic model are demonstrated by applying it to the flapping dynamics of an articulated helicopter rotor blade. The influence of unsteady aerodynamics on the damping characteristics of the rotor is examined. The same problem is also treated by using a different unsteady aerodynamic model, namely dynamic inflow. Based on a comparison of the results obtained with these two unsteady aerodynamic models, useful conclusions are drawn regarding some fundamental features of these theories.

Nomenclature

a	= Lift curve slope
a_i, b_i	= Coefficients in approximate aerodynamic transfer function
b	= Blade semichord
$C(k)$	= Theodorsen's lift deficiency function
$C(\bar{s})$	= Generalized Theodorsen's lift deficiency function
C'	= Loewy's lift deficiency function
C'_{eq}	= Equivalent lift deficiency function
C'_{DI}	= Lift deficiency function obtained using dynamic inflow model

* This research was supported by NASA Grant NAG 2-209, funded by NASA Ames Research Center, Moffett Field, California

† Professor of Engineering and Applied Science

†† Assistant Research Engineer

C_L' = Low frequency approximate transfer function for Loewy's lift deficiency function

C_T = Thrust coefficient

C_{MY}, C_{MX} = Pitch and roll moment coefficients, respectively

F,G = Real and imaginary parts of Theodorsen's lift deficiency function, $C = F + iG$

F',G' = Real and imaginary parts of Loewy's lift deficiency function $C' = F' + iG'$

$\bar{F}(t)$ = Unsteady aerodynamic force at the blade root

$G(i\omega)$ = Transfer function

$H_n^2(k)$ = Hankel functions of second kind of order n; $H_n^2 = J_n - iY_n$

$\bar{h}_e$ = Equivalent wake spacing; $\bar{h}_e = \frac{2\pi U_{p0}}{Q\Omega b}$

I_b = Moment of inertia of the blade about the flap hinge

$J_n(k)$ = Bessel functions of first kind of order n

k = Reduced frequency, $k = \frac{\omega b}{\Omega r}$ or $\frac{\omega b}{u}$

L = Lift per unit span of the blade

L_c = Circulatory lift on the airfoil

$\bar{m}_e$ = Equivalent frequency ratio; $\bar{m}_e = \frac{\omega}{\Omega Q}$

M = Aerodynamic flap moment

$\bar{M}$ = Steady part of the aerodynamic flap moment

$\Delta M(t)$ = Time varying part of the aerodynamic flap moment

ΔM_m = Collective flap moment coordinate

M_1 = Nondimensional apparent mass associated with inflow variable λ_1

p = Eigenvalue; $p = \bar{\sigma} \pm i\,\bar{\omega}$

Q = Number of blades in a rotor or 3/4-chord-downwash velocity

$\bar{r}_{eq}$ = Representative radial station on the blade for unsteady effects

$\bar{r}_e$ = Radial station for the typical blade section, $\bar{r}_e = \frac{r}{bQ}$

R = Rotor radius

s = Laplace variable

$\bar{s}, \tilde{s}$ = Nondimensional Laplace variables; $\bar{s} = \frac{b}{\Omega 0.75R} s$; $\tilde{s} = \frac{s}{\Omega}$; $\bar{s} = \frac{b}{U} s$

U = Free stream velocity

U_{P0} = Induced velocity normal to the rotor disk

β_0 = Steady flap angle

β_k = Flap coordinate of the k^{th} blade

$\Delta\beta_k$ = Time varying part of the flap angle, for k^{th} blade

$\Delta\beta_m$ = Collective flap coordinate of the rotor

γ = Lock number; $\gamma = \frac{2\rho abR^4}{I_b}$

λ_0 = Steady inflow; $\lambda_0 = \frac{U_{p0}}{\Omega R}$

$\lambda_1, \lambda_{1c}, \lambda_{1s}$ = Inflow variables

$\delta\lambda$ = Perturbational inflow

λ = Total Inflow; $\lambda = \lambda_0 + \delta\lambda$

ω = Frequency

$\bar{\omega}$ = Complex part of the eigenvalue p

Ω = Rotor angular speed

ψ = Azimuthal angle or nondimensional time, $\psi = \Omega t$

ρ = Density of air

$\bar{\sigma}$ = Real part of the eigenvalue p

σ = Solidity ratio

τ = Nondimensional time; $\tau = \frac{0.75R}{b} \Omega t$

$\phi_{F.W}(\tau)$ = Fixed wing indicial response function

$\phi_{R.W}(\tau)$ = Rotary wing indicial response function

$\dot{(\ )}$ = Derivative with respect to time t

$(*)$ = Derivative with respect to nondimensional time Ωt

1. Introduction

It is well known that unsteady aerodynamics plays an important role in the aeroelastic stability and response calculation of both fixed wing and rotary-wing vehicles. However most rotary wing aeroelastic analyses use either quasi-steady aerodynamic theories or two dimensional theories which are based on the assumption that the airfoil is undergoing simple harmonic motions (such a theory is denoted frequency domain theory in this paper). These restrictive aerodynamic assumptions were due primarily to the lack of suitable unsteady aerodynamic models in the time domain. Representative theories which are based on the assumption of simple harmonic airfoil motions are: (a) Theodorsen's[1] incompressible two-dimensional unsteady aerodynamic theory and Greenberg's[2] extension of Theodorsen's theory which accounts for pulsating oncoming flow velocity and constant angle of attack; these theories have been developed for fixed wings, however, they have also been used frequently in rotary-wing applications and, (b) Loewy's theory[3] and Shipman and Wood's theory[4], which are applicable to a helicopter rotor in hover and forward flight, respectively. Theodorsen's theory for fixed wings assumes a planar wake behind the airfoil extending to infinity, whereas Loewy's theory for rotary wings assumes an unsteady wake behind and beneath the reference airfoil extending, to infinity in both directions, as shown in Figure 1.

These theories have a significant limitation when applying them to aeroelastic stability calculations, since the assumption of simple harmonic motion, upon which they are based, implies that they are strictly valid only at the stability boundary, and thus they provide no information on system damping before or after the flutter condition is reached. Thus standard stability analyses, such as the root locus method, cannot be used in conjunction with these theories. Another important limitation of these theories is evident when one tries to apply them to the rotary-wing aeroelastic problem in forward flight, which is governed by equations with periodic coefficients. In this case the complex lift deficiency function associated with frequency domain unsteady aerodynamics is not consistent with the numerical methods employed in the treatment of periodic systems. Furthermore these unsteady aerodynamic theories are not suitable for the analysis of aeroelastic systems with active controls, such as higher harmonic control devices and the transient response analysis of aeroelastic systems, such as rotor blade response in forward flight. Thus there is a need for unsteady aerodynamic theories which are capable of modeling the unsteady aerodynamic loads, in time domain for finite time arbitrary motion of an airfoil, representing the cross-section of an oscillating helicopter rotor blade. It should be noted that in this paper the term arbitrary motion is used to denote growing or decaying oscillations with a certain frequency.

Such an unsteady aerodynamic theory for finite time arbitrary motion of an airfoil has been developed recently for fixed wing applications[5]. However the success in developing similar theories which are suitable for rotary wing applications has been somewhat limited.

A clear description of the historical development of the application of Laplace transform techniques to the problem of unsteady aerodynamics for finite time arbitrary airfoil motions can be found in References 5 and 6. Recently Edwards[5] showed that the Laplace transform of the circulatory load

on an airfoil, executing arbitrary motion in incompressible flow, is related to the product of the Laplace transform of the generalized Theodorsen function $C(\bar{s})$ and the Laplace transform of the 3/4-chord downwash velocity of the airfoil. The generalized Theodorsen lift deficiency function $C(\bar{s})$, in the Laplace domain, is equivalent to replacing, ik, in Theodorsen's lift deficiency function C(k) by the nondimensional Laplace transform variable $\bar{s}$.

Since the value of Theodorsen's lift deficiency function is known exactly in the frequency domain, Vepa[7] represented C(k) by a ratio of two polynomials $C(k) = N(ik)/D(ik)$, where N(ik) and D(ik) were equal degree polynomials. Vepa evaluated the coefficients in these polynominals by a least squares technique and obtained very good approximations to C(k). An alternative procedure for obtaining approximate expressions for C(k) was proposed by Dowell[8]. Dowell's technique is based on a parameter identification technique in which the time history of the aerodynamic load on the airfoil was assumed to consist of sums of exponentials. Applying the fundamental correspondence between the frequency domain and time domain aerodynamic loads, Dowell evaluated the time constants and the coefficients which provide the best fit to the frequency domain representation of the aerodynamic forces. It should be noted that Dowells' procedure is based on the assumption that the functional form of the indicial response function is known apriori. The approximate representations of Theodorsen's lift deficiency function C(k), obtained by Vepa or Dowell, can be used to model the unsteady aerodynamic loads produced by completely arbitrary, small, time dependent motion of an airfoil. Since these approximate transfer functions for C(k) are finite degree polynomials, they are also referred to as finite state models for the unsteady aerodynamics.

More recently, in Ref. 6 and 9, Greenberg's theory and Loewy's theory, which are representative of unsteady aerodynamic theories frequently used in rotary-wing aeroelasticity, have been also generalized for arbitrary motions. The generalization of Greenberg's theory is straightforward[9] and could be done along the lines indicated in Ref. 5. In Ref. 9, Dinyavari and Friedmann, generalized the Loewy's lift deficiency function C' by replacing ik in the lift deficiency function by the non-dimensional Laplace variable $\bar{s}$. Following Dowell's[8] procedure, a finite state Pade approximation to Loewy's lift deficiency function was obtained. However this approximation failed to capture the oscillatory behavior of Loewy's lift deficiency function, which is a special feature of the unsteady aerodynamic loads acting on a rotor blade.

This paper has a number of objectives: (a) Formulation of a new technique for approximating rotary-wing lift deficiency functions, such as Loewy's, which are oscillatory in nature, so as to be able to extend such theories to arbitrary motions in the time domain; (b) Present the methodology needed for applying finite-time arbitrary motion unsteady aerodynamic theory to a helicopter rotor dynamic problem and (c) Treat the same rotor dynamic problem using dynamic inflow and compare some of the fundamental features of these theories.

First a new technique for identifying and formulating the mathematical form of the finite unsteady aerodynamic transfer function by utilizing Bode Plot method[10], is presented. Then using the finite state unsteady aerodynamic models, the indicial response functions for both the rotary wing and fixed wing case are obtained. It is shown that the rotary wing indicial response function is qualitatively different in nature when compared to the fixed wing indicial

response function. For fixed wings, the indicial response function exhibits a steady exponential decaying form whereas for rotary wings the indicial response function has an oscillatory form with exponential decay. Therefore, the rotary wing indicial response overshoots the steady value at certain specific times. This feature of the rotary wing indicial response function has been also observed experimentally[11]. In Ref. 11, it was found experimentally that the thrust response of a rotor to a sudden change in the collective setting of the blades overshoots the steady state value prior to reaching it.

Subsequently the finite state unsteady aerodynamic model is applied to a rotor dynamic problem, in which the effects of unsteady aerodynamics on the flap damping and frequency of the rotor are evaluated. The same aeroelastic problem is also studied using a different unsteady aerodynamic model, namely the dynamic inflow model. The results obtained with these two unsteady aerodynamic models are compared. From this comparison certain conclusions on the fundamental nature of finite state unsteady aerodynamic models and their relation to dynamic inflow models are drawn.

2. Brief Description of the Bode Plot and Its Role in Unsteady Aerodynamics Modeling

One of the methods frequently used in the analysis and design of control systems is the frequency response method. When using this method, the frequency of the input is varied over a wide range and the resulting output response is studied. Using this method, the transfer functions of complicated systems can be determined. This particular aspect of determining the transfer function from the frequency response curve can also be used to formulate approximate transfer functions for the unsteady aerodynamics of a two-dimensional airfoil oscillating in incompressible flow. Furthermore, the method is equally applicable to both fixed wing type or rotary wing type of unsteady aerodynamic theories where the lift deficiency function plays the role of a transfer function, which relates the 3/4-chord downwash velocity to the aerodynamic load acting on the airfoil. Since lift deficiency functions, such as Theodorsen's for the fixed wing case and Loewy's for the rotary wing case are known exactly for simple harmonic motion of the airfoil, the approximate transfer functions can be formulated by applying frequency-response techniques used in control system engineering.

One of the methods used for representing the frequency-response of a transfer function is the Bode diagram[10]. The Bode diagram consists of two graphs. One is a plot of the logarithm of the magnitude of the sinusoidal transfer function and the other is a plot of the phase angle. Both are plotted as a function of frequency on a logarithmic scale. For the present application only a plot of the magnitude versus frequency is needed and therefore we shall restrict our attention to this particular aspect of the Bode plot. This portion of the Bode plot consists of logarithmic magnitude of the transfer function $G(i\omega)$, i.e., $20 \log|G(i\omega)|$ versus the frequency ω.

Since our aim is to formulate an approximation to the transfer function represented by the unsteady lift deficiency function we seek the information about the qualitative nature of the poles and zeros, i.e., whether they are real or complex and where they are located. This information can be obtained by analyzing the Bode plot of the lift deficiency function. A detailed description of the features of the bode plots and its asymptotic properties,

which are useful in this regard can be found in Refs. 10 and 14, and for the sake of conciseness are not repeated here. The most important properties of the Bode plots, which are needed for our application are summarized below.

(a) A +20 db/decade change in slope in the asymptotes is indicative of the presence of a real zero and a -20 db/decade change in slope indicates the presence of a real pole in the transfer function;

(b) peaks in the Bode plot indicate the presence of complex poles and complex zeros in the transfer function;

(c) a -40 db/decade change in slope in the asympototes indicates the presence of either complex poles or two equal real poles and a +40 db/decade change in slope indicates the presence of either complex zeros or two equal real zeros;

(d) whenever the slopes of the asymptotes of the transfer function are equal, at low or at high frequencies, then the transfer function has an equal number of poles and zeros.

These properties are very useful when one attempts to construct approximation to the lift deficiency function, which has the role of an aerodynamic transfer function in unsteady aerodynamics.

3. Finite State Modelling of Theodorsen's Lift Deficiency Function

Theodorsen's lift deficiency function, for a two dimensional airfoil executing simple harmonic motion in incompressible flow, is given in exact form by[12]

$$C(k) = \frac{H_1^2(k)}{H_1^2(k) + iH_0^2(k)} \tag{1}$$

The real and imaginary parts of C(k) are shown in Fig. 2. A Bode plot of Theodorsen's lift deficiency function is presented in Fig. 3. It can be seen from Fig. 3 that the low frequency and the high frequency asymptotes have equal slopes with a value of 0 db/decade. Furthermore the Bode plot does not show any peaks and the slope of the exact curve at any point is less than -20 db/decade. Therefore, using the general properties of the Bode plots summarized before, the approximate transfer function for C(k) must have an equal number of poles and zeros, which are real. Based on these considerations, a third degree polynomial approximation for C(k), in the form of

$$C(k) \cong \frac{0.5(ik + a_1)(ik + a_2)(ik + a_2)}{(ik + b_1)(ik + b_2)(ik + b_3)} \tag{2}$$

can be assumed. The transfer function satisfies the condition that C(k) approaches 0.5 as k approaches infinity. Imposing the constraint that C(k) = 1 for k = 0, the coefficients a_1, a_2, a_3, b_1, b_2, b_3 are determined by a least square technique, whereby the real and imaginary parts of the transfer function are set equal to the real and imaginary parts of the exact function C(k). The approximate function obtained in this manner is given by

$$C(k) \cong \frac{(0.5(ik + 0.088)(ik + 0.37)(ik + 0.922)}{(ik + 0.072)(ik + 0.261)(ik + 0.80)} \qquad (3)$$

The real and imaginary parts of the exact C(k) function together with the approximate transfer function, given by Eq. (13), are shown in Fig. 2. It can be seen that the [3.3] polynomial approximation gives an excellent agreement with the exact values of the Theodorsen lift deficiency function* C(k). The location of the poles (p_1,p_2,p_3) and zeros (z_1,z_2,z_3) and the asymptotic behavior of the approximate transfer function, given by Eq. (3), are shown in Fig. 3. It is evident from Fig. 3 that the poles and zeros of the approximate transfer function lie in a range of reduced frequencies k where the Bode plot of the exact transfer function has a higher slope then at other values of k, i.e., $0.06 \leq k \leq 1.0$. This particular feature associated with the location of the poles and zeros is very useful for estimating their initial values required for constructing the approximate transfer function by the nonlinear least squares technique.

Using the approximate transfer function obtained for Theodorsen's lift deficiency function C(k), the indicial response function can be obtained by taking the inverse Fourier transform of the approximate transfer function[12]. The indicial response function obtained for the [3.3] polynomial approximation given by Eq. (3) is

$$\phi_{F.W.}(\tau) \cong 1.0 - 0.203\ e^{-0.072\tau} - 0.236\ e^{-0.261\tau} - 0.06\ e^{-0.8\tau} \qquad (4)$$

4. Finite State Modelling of Loewy's Lift Deficiency Function

Loewy's rotary wing unsteady airfoil theory represents an approximation to the unsteady aerodynamic loads acting on a rotor blade cross section in hover. The effects of the spiral returning wake beneath the rotor, shown in Fig. 1, are considered in an approximate manner. These wake layers represent wakes shed by other blades, as well as the reference blade in previous revolutions. The wake layers extend to infinity before and behind the reference airfoil. Loewy's theory is intended for lightly loaded rotors (i.e. low inflow conditions) and like Theodorsen's theory it is also based on the assumption of simple harmonic motion of the reference airfoil.

Loewy's lift deficiency function, in the frequency domain, for the collective mode of the rotor, where all the blades move in phase, is given by[13]

$$C'(k,\bar{m}_e,\bar{h}_e) = \frac{H_1^2(k) + 2J_1(k)\ W(k\bar{h}_e,\bar{m}_e)}{H_1^2(k) + i\ H_0^2(k) + 2[J_1(k) + iJ_0(k)]\ W(k\bar{h}_e,\bar{m}_e)} \qquad (5)$$

*Since the two curves coincide in Fig. 2.

where the wake weighting function W is given by

$$W(k\bar{h}_e, \bar{m}_e) = \begin{cases} \dfrac{1}{e^{k\bar{h}_e}\, e^{i2\pi\, \bar{m}_e} - 1} & k > 0 \\ 0 & k = 0 \end{cases} \qquad (6)$$

The quantities $\bar{h}_e$, $\bar{m}_e$ for a typical blade section at a radial distance r from the axis of rotation, for a rotor with Q blades, are defined as

$$\bar{m}_e = \frac{\omega}{\Omega Q} = \frac{\omega b}{\Omega r} \cdot \frac{r}{Qb} = k\,\bar{r}_e$$

$$\bar{r}_e = \frac{r}{Qb}$$

$$\bar{h}_e = \frac{2\pi U_{p0}}{\Omega Q b} = \frac{2\pi U p_0}{\Omega R} \cdot \frac{R}{Qb} = \frac{2\pi\lambda_0}{Q(b/R)}$$

In the definition of the equivalent frequency ratio $\bar{m}_e$, it should be noted that for a given blade section at a radial station r from the axis of rotation, $\bar{m}_e$ is dependent on the reduced frequency k.

We shall show that the technique based on the Bode plot, developed in this paper, is successful in formulating the approximate transfer function for the Loewy's lift deficiency function. To illustrate the method, the following example was selected. The trust coefficient is $C_T = 0.005$ and the blade section is taken at 0.75R. The rotor was assumed to have four blades and the blade semichord is b = 0.024R. The corresponding inflow ratio is calculated from $\lambda_0 = \sqrt{C_T/2} = 0.05$ and the values of $\bar{h}_e$ and $\bar{r}_e$ are given by $\bar{h}_e = 3.2725$ and $\bar{r}_e = 7.8125$, respectively. This example is representative of a typical helicopter application. The typical blade section was taken to be at 75% of the span due to the following considerations. First it is common practice to consider the blade section at 0.75R to be representative of rotor aerodynamic behavior under steady conditions. Secondly, to justify this assumption under unsteady conditions the unsteady aerodynamic loads, at twenty spanwise stations, were evaluated for a blade undergoing simple harmonic flapping motion. These loads were computed using Loewy's exact lift deficiency function. The loads were integrated along the blade span to obtain the unsteady aerodynamic thrust and the moment at the blade root. These calculations were performed at various flap frequencies, in the range of 1/rev ~ 2/rev. The details of this calculation can be found in Ref. 14. For all cases considered the integral value of the unsteady aerodynamic loads at the root indicated that the unsteady aerodynamic load at 75% span is indeed a suitable representative value, without any loss of accuracy. Once a finite state model for the unsteady aerodynamic transfer function is formulated for this particular blade section, the same model is also applicable to other blade sections along the span.

Figure 4 illustrates the real (F') and imaginary (G') parts of Loewy's exact lift deficiency function for this case. From Fig. 4 it is evident that the real and imaginary parts of the Loewy's lift deficiency function are

highly oscillatory. The Bode plot of Loewy's lift deficiency function is presented in Fig. 5. The Bode plot has many peaks and valleys. Hence the corresponding approximate lift deficiency or transfer function which we seek, must have as many complex poles and complex zeros as there are peaks and valleys in the Bode plot. In Fig. 5 the odd numbers, corresponding to the valleys, indicate complex zeros and the even numbers, corresponding to the peaks, indicate complex poles. For practical situations high reduced frequencies above $k \geq 1$ are not feasible. Therefore the approximate transfer function is constructed so as to capture the first eight complex poles and complex zeros. This approximate transfer function can be written in the following form

$$C'(k,\bar{h}_e,\bar{m}_e) \cong F' + G' = \frac{0.5(ik+a_1)}{(ik+b_1)} \prod_{j=1}^{8} \frac{[(ik)^2+a_{2j}\ ik+a_{2j}+1]}{[(ik)^2+b_{2j}\ ik+b_{2j}+1]} \tag{7}$$

The task of evaluating the 34 coefficients $a_1 \ldots a_{17}$ and $b_1 \ldots b_{17}$ by a nonlinear least squares technique leads to a problem which converges slowly. To facilitate the numerical calculations the problem was modified so that the coefficients could be evaluated by solving a linear least squares problem. For this case the approximate lift deficiency function is given by

$$C' = F' + iG' \cong 0.5\ \frac{(ik)^{17} + a_1(ik)^{16} + \ldots + a_{17}}{(ik)^{17} + b_1(ik)^{16} + \ldots + b_{17}} = \frac{N(ik)}{D(ik)} \tag{8}$$

The coefficients $a_1 \ldots a_{17}$, $b_1 \ldots b_{17}$ are evaluated by minimizing the error $\sum_{M=1}^{N} [C'\, D(ik_M) - N(ik_M)]^2$. The coefficients obtained from this procedure[14] are given in Table I. Table II gives all the poles and zeros of the approximate transfer function represented by Eq. (8). It can be seen that, for this case, there are eight complex poles and eight complex zeros, in addition to one real pole and a real zero.

In Fig. 4, the real and imaginary parts of the approximate lift deficiency or transfer function, given by Eq. (8), are compared with Loewy's exact lift deficiency function. It is evident that the agreement between the two sets of curves is very good.

Recall that from linear, incompressible, two dimensional unsteady aerodynamic theory Wagner's indicial response function and Theodorsen's lift deficiency function are related by a Fourier transform[12]. Loewy's theory is the rotary-wing counterpart of Theodorsen's theory. Therefore by analogy the rotary-wing indicial response function and Loewy's lift deficiency function can be also related by the Fourier transform given below

$$\phi_{R.W.}(\tau) = \frac{1}{2\pi} \int_{-\infty}^{\infty} \frac{C'(ik)}{ik}\ e^{ik\tau}\, dk \tag{9}$$

The approximate transfer function, given in Eq. (8), can be substituted in Eq. (9) for C'. Applying partial fractions and using a table of inverse Laplace transforms, the approximate rotary-wing indicial response function $\phi_{R.W.}(\tau)$ was calculated[14] and is depicted in Fig. 6. It can be seen from Fig. 6 that the indicial response is oscillatory and at certain values of τ the response overshoots the steady value 1.0. This result implies that for a step change in angle of attack of the rotor blade the thrust developed by the rotor will overshoot the steady value before reaching it. This phenomenon has been experimentally observed in Ref. 11. The authors of Ref. 11 noted that for a rapid change in collective pitch setting of a model rotor, the measured thrust overshoots its steady state value. This is precisely the qualitative nature of the indicial response function $\phi_{R.W.}(\tau)$ shown in Fig. 6.

In general, the rotary wing indicial response function can be written as[14]

$$\phi_{R.W.}(\tau) \cong 1.0 - \sum_{j=1}^{N} e^{-b_j\tau} [A_j \cos \omega_j\tau + B_j \sin \omega_j\tau] \tag{10}$$

The values of A_j, B_j and b_j's depend on the rotor geometry and the rotor operating conditions and can be evaluated from the approximate transfer function corresponding to Loewy's lift deficiency function, defined for that specific rotor. It should be also noted that this is the first time that the mathematical form of a rotary wing indicial response function is presented in the literature.

Recall from the previous discussion of the fixed wing case that the indicial response function can be written as

$$\phi_{F.W.}(\tau) \cong 1.0 - \sum_{j=1}^{N} A_j e^{-b_j\tau} \tag{11}$$

Comparing the rotary wing indicial response functions $\phi_{R.W.}$, Eq. (10), with the fixed wing indicial response function $\phi_{F.W.}$, Eq. (11), it can be concluded that the rotary-wing indicial response function is qualitatively different from the fixed wing indicial response function. The rotary wing indicial response function exhibits an oscillatory nature whereas the fixed wing indicial response is nonoscillatory.

5. Influence of Unsteady Aerodynamics on the Flapping Dynamics of a Helicopter Rotor

In this section finite state unsteady aerodynamics are applied to a simple rotor dynamic problem. In particular we wish to clarify three important items: (a) illustrate the methodology of applying finite state unsteady aerodynamics to a rotor dynamic problem; (b) evaluate the effects of unsteady aerodynamics on the damping and frequency of rotor flapping dynamics; and (c) compare the results obtained using the unsteady aerodynamic model developed in this study, with results obtained using dynamic inflow, for the same rotor dynamic problem.

5.1 Application of a Generalized Loewy Theory to Rotor Flapping Dynamics

From the review of the pertinent literature it is evident that the only case when finite state unsteady aerodynamics was applied to a rotor dynamic problem was presented in Refs. 6 and 15, where a generalized Greenberg theory was used. Here we apply a generalized Loewy theory for the first time to a rotor dynamic problem, and therefore we use a relatively simple example which is adequate for illustrative purposes. The example rotor consists of four uniform blades which are articulated and centrally hinged. Each blade is assumed to have only a flap degree of freedom. The rotor is in hover, with $C_T = 0.005$ and the blade semichord is $b/R = 0.024$. Furthermore we restrict our attention to the collective flap degree of freedom for which approximate lift deficiency function was evaluated in the previous section and we shall determine the influence of unsteady aerodynamics on the damping and frequency of the perturbational flapping motion of the rotor.

The first step in solving this rotor dynamic problem is to generalize the approximate transfer function for Loewy's lift deficiency function, given in Eq. (8), to arbitrary motion of the airfoil. This is accomplished by replacing (ik) in Eq. (8) by the nondimensional Laplace variable $\bar{s}$. The generalized lift deficiency function is given by

$$C' \cong 0.5 \frac{\bar{s}^{17} + a_1\bar{s}^{16} + \text{-----} + a_{17}}{\bar{s}^{17} + b_1\bar{s}^{16} + \text{-----} + b_{17}} \tag{12}$$

The values of the coefficients a_1 --- a_{17}, b_1 --- b_{17} are given in Table I.

The fundamental natural frequency of a centrally hinged articulated blade is 1/rev. Therefore the corresponding reduced frequency k, for the typical blade section at 0.75 R, with a semichord of $b/R = 0.024$ is

$$k = \frac{\omega b}{\Omega r} = \frac{\omega}{\Omega} \frac{b}{.75R} = 0.032$$

This value of the reduced frequency is very small. Therefore by restricting the validity of the approximation to low values of k, i.e. $0 \leq k \leq 0.05$, a further approximation of Eq. (12) is possible. An approximation which is valid for such low frequencies can be written as

$$C' = 0.50 \left[\frac{a_{16}\bar{s} + a_{17}}{b_{16}\bar{s} + b_{17}} \right] \tag{13}$$

Having obtained such a first order approximation, to the generalized lift deficiency function, it can be incorporated in the dynamic problem of a flapping rotor. This simplified model enables one to determine the influence of unsteady aerodynamics, at low reduced frequencies, on the flapping response of a rotor.

Neglecting apparent mass terms the lift on a typical section of the rotor blade, located at a radial station r from the axis of rotation, is given by

$$L(t) = \rho a\, b \Omega r\, \mathcal{L}^{-1}\, [C'(\bar{s})Q(s)]\, dr \tag{14}$$

where $C'(\bar{s})$ is given by Eq. (13) and Q(s) is the Laplace transform of the 3/4-chord downwash velocity. Define a new function T(t) given by

$$T(t) = \mathcal{L}^{-1}\, [C'(\bar{s})Q(s)] \tag{15}$$

The function T(t) can be considered to be representative of the circulation around the airfoil. Substituting Eq. (15) in Eq. (14), the lift on the blade section becomes

$$L(t) = \rho a\, b \Omega r\, T(t)\, dr \tag{16}$$

The equation of motion of the k^{th} blade in the flap degree of freedom is[13]

$$I_b\, \ddot{\beta}_k + I_b\, \Omega^2\, \beta_k = \int_0^R L(t)\, r\, dr \tag{17}$$

where $I_b = \int_0^R r^2 m dr$. Combining Eqs. (16) and (17) yields

$$I_b\, \ddot{\beta}_k + I_b\, \Omega^2\, \beta_k = \int_0^R \rho a\, b \Omega r^2\, T(t)\, dr = M(t) \tag{18}$$

where M(t) is the aerodynamic moment about the root hinge.

Multiplying both sides of Eq. (16) by $\rho a \Omega b r^2 dr$, integrating over the blade, and taking the Laplace transform of the final expression yields

$$\int_0^R \rho a\, b \Omega T(s)\, r^2 dr = \int_0^R \rho a\, b \Omega r^2\, C'(\bar{s})Q(s) dr \tag{19}$$

In Eq. (19) the integration is over r, thus the lift deficiency function $C'(\bar{s})$ can be taken outside the integral. Substituting for $C'(\bar{s})$ from Eq. (13) and recognizing that the left hand side of Eq. (19) is the Laplace transform of the aerodynamic moment M, one can manipulate Eq. (19) to yield[14]

$$(b_{16}\bar{s} + b_{17})\, M(s) = \rho a\, b\, \Omega \int_0^R 0.5\, (a_{16}\bar{s} + a_{17})\, Q(s) r^2 dr \tag{20}$$

Replacing the nondimensional Laplace variable $\bar{s}$ by the dimensional Laplace variable s, where $\bar{s} = bs/(0.75\, \Omega R)$ and taking the inverse Laplace transform of Eq. (20) yields

$$b_{16}\frac{b}{\Omega 0.75R}\dot{M} + b_{17}M = \rho a b \Omega \int_0^R 0.5\left(a_{16}\frac{b}{\Omega 0.75R}\dot{Q} + a_{17}Q\right) r^2 dr \quad (21)$$

The downwash velocity at the 3/4 chord can be written as[9]

$$Q(t) = \Omega r\left[\theta_0 + \Delta\theta(t)\right] - r\dot{\beta}_k - \lambda_0 \Omega R + b(\tfrac{1}{2} - \bar{a})\Delta\dot{\theta}$$

Assuming that the blade pitch angle is constant, i.e., $\Delta\theta = \Delta\dot{\theta} = 0$, the downwash velocity Q becomes

$$Q(t) = \Omega r\,\theta_0 - r\dot{\beta}_k - \lambda_0\,\Omega R \quad (22)$$

Substutiting Eq. (22) in Eq. (21) and integrating over the blade span yields

$$b_{16}\frac{b}{\Omega 0.75R}\dot{M} + b_{17}M = 0.5\,\rho a b \Omega\left\{a_{16}\frac{b}{\Omega 0.75R}\left(-\frac{R^4}{4}\ddot{\beta}_k\right) + a_{17}\left(\underline{\frac{R^4}{4}\Omega\theta_0} - \frac{R^4}{4}\dot{\beta}_k - \Omega\underline{\frac{R^4}{4}\lambda_0}\right)\right\} \quad (23)$$

Equations (18) and (23) are two equations which have to be solved simultaneously to determine the influence of unsteady aerodynamics on the flap motion of the blade. The right hand side of Eq. (23) consists of a constant part, which is underlined, and a time varying part. Therefore the solutions for M and hence β_k can be written as

$$M = \bar{M} + \Delta M(t)$$

$$\beta_k = \beta_0 + \Delta\beta_k(t) \quad (24)$$

where M and β_0 represent the steady parts and ΔM, $\Delta\beta_k$ represent the time varying parts.

Substituting Eq. (24) in Eqs. (23) and (18) and using the relation, $a_{17} = 2b_{17}$ as given in Table I, one can separate the steady and time varying parts of the moment and flapping angle. The steady part of the moment $\bar{M}$ is given by

$$\bar{M} = \rho a b \Omega^2 R^4\left(\frac{\theta_0}{4} - \frac{\lambda_0}{3}\right) \quad (25)$$

and the steady part of the flap angle β_0 is

$$\beta_0 = \frac{\gamma}{2}\left(\frac{\theta_0}{4} - \frac{\lambda_0}{2}\right) \quad (26)$$

where $\gamma = 2\rho a\, b\, R^4/I_b$. These expressions for $\bar{M}$ and β_0 agree with conventional results given in Ref. 13. The equations for the time varying parts ΔM and $\Delta\beta_k$ in nondimensional form are given by

$$\overset{**}{\Delta\beta}_k + \Delta\beta_k = \frac{\Delta M}{I_b \Omega^2} = \overline{\Delta M} \tag{27}$$

$$b_{16} \frac{b}{0.75R} \overset{*}{\overline{\Delta M}} + b_{17} \overline{\Delta M} = -\frac{\gamma}{16} \left[a_{16} \frac{b}{0.75R} \overset{**}{\Delta\beta}_k + a_{17} \overset{*}{\Delta\beta}_k\right] \tag{28}$$

The flap equation and the aerodynamic moment equation, Eqs. (27) and (28), are the same for all the blades in the rotor. After applying the multiblade coordinate transformation[13] to the flap degree of freedom and assuming that the same transformation is also valid for the unsteady aerodynamic moment $\overline{\Delta M}$, the collective flap and collective moment equations become,

$$\overset{**}{\Delta\beta}_m + \Delta\beta_m = \overline{\Delta M_m} \tag{29}$$

$$b_{16} \frac{b}{0.75R} \overset{*}{\overline{\Delta M}_m} + b_{17} \overline{\Delta M_m} = -\frac{\gamma}{16} \left[\frac{b}{0.75R} a_{16} \overset{**}{\Delta\beta}_m + a_{17} \overset{*}{\Delta\beta}_m\right] \tag{30}$$

The influence of unsteady aerodynamics on the collective flap mode of the rotor can be determined from an eigenanalysis of the system represented by Eqs. (29) and (30).

Consider first a zeroth order approximation to the generalized Loewy lift deficiency function, i.e. assume $a_{16} = b_{16} = 0.0$ in Eq. (30). For this case the collective flap equation, Eq. (30), reduces to

$$\overset{**}{\Delta\beta}_m + \Delta\beta_m = -\frac{\gamma}{8} \overset{*}{\Delta\beta} \tag{31}$$

which represents flap mode dynamics in presence of quasi-steady aerodynamics. The eigenvalues corresponding to the collective flap mode, for $\gamma = 8.0$, are $p = \bar{\sigma} \pm i\,\bar{\omega} = -0.5 \pm i\,0.866$. The quantity $\bar{\sigma} = -0.5$ represents the flap damping and $\bar{\omega} = 0.866$ refers to the nondimensional flap frequency.

The influence of unsteady aerodynamics on flap damping is considered next. Substituting the values of a_{16}, a_{17}, b_{16}, b_{17} from Table I, in Eq. (30) it becomes

$$0.04288 \overset{*}{\overline{\Delta M}}_m + 0.16 \overline{\Delta M_m} = -\frac{\gamma}{8} \left[0.02672 \overset{**}{\Delta\beta}_m + 0.16 \overset{*}{\Delta\beta}_m\right] \tag{32}$$

Solving Eqs. (29) and (32) for $\gamma = 8.0$, yields the following eigenvalues $p_1 = -3.252$ and $p_{2,3} = -0.551 \pm i\,0.919$. The eigenvalue $p_1 = -3.252$ corresponds to the unsteady aerodynamic moment. The eigenvalues corresponding to the collective flap mode are $p_{2,3} = -0.551 \pm i\,0.919$. Comparing

these values with the results obtained with quasi-steady aerodynamics, it is evident that unsteady aerodynamics increases flap damping by 10% and the flap frequency by 6%. When unsteady aerodynamics are included the aerodynamic lift on the airfoil lags behind the airfoil motion, which causes an increase in flap damping. The lag of the aerodynamic lift is due to the negative sign of the imaginary part G' in Loewy's lift deficiency function, as shown in Fig. 4.

The influence of unsteady aerodynamics in rotor dynamic problems is equivalent to a modification of the Lock number. Taking the Laplace transform of Eqs. (29) and (32) and substituting for $\Delta M_m(\tilde{s})$ in terms of $\Delta\beta_m(\tilde{s})$ in Eq. (29), one obtains

$$\left\{ \tilde{s}^2 + 1 + \frac{\gamma}{8} \underline{\left[\frac{0.02672\ \tilde{s} + 0.16}{0.04288\ \tilde{s} + 0.16} \right]} \tilde{s} \right\} \Delta\beta_m(\tilde{s}) = 0 \qquad (33)$$

where s is the nondimensional Laplace variable $\tilde{s} = \frac{s}{\Omega}$ and the relation between $\tilde{s}$ and $\bar{s}$ is given by $\bar{s} = \frac{b}{0.75R}\ \frac{s}{\Omega} = \frac{b}{0.75R}\ \tilde{s}$. The underlined term in Eq. (33) represents a modified Lock number, which can be written as

$$\gamma^* = \gamma \left[\frac{0.02672\ \tilde{s} + 0.16}{0.04288\ \tilde{s} + 0.16} \right] = \gamma C_L'(\tilde{s}) \qquad (34)$$

where $C_L'(\tilde{s})$ is a low frequency approximation to Loewy's lift deficiency function. Substituting the values of a_{16}, a_{17}, b_{16} and b_{17}, from Table I, into Eq. (13) and modifying $\bar{s}$ to $\tilde{s}$, the low frequency approximation to Loewy's deficiency function, given by Eq. (34) can be obtained.

5.2 Application of the Dynamic Inflow Model to Rotor Flapping Dynamics

The rotor dynamic problem treated in the previous section can be also re-examined using a different low frequency approximation of unsteady aerodynamics known as the dynamic inflow model.

A detailed description of the dynamic inflow model frequently employed in rotor dynamic and aeroelastic calculations, can be found in Refs. 13, 16 and in a more condensed manner also in Ref. 17. Dynamic inflow is a simple model which represents approximately the unsteady effects of the rotor wake. The unsteady wake-induced flow through the rotor disk is defined by a set of inflow variables which provide a correction to the inflow assumed in a quasi-steady aerodynamic theory. The total induced velocity on the rotor disk due to the wake is assumed to consist of two parts: (1) a steady inflow λ_0 (for trim loading) and (2) a perturbation inflow $\delta\lambda$(for transient loading). Therefore, the total induced flow normal to the rotor disk can be expressed as

$$\lambda = \lambda_0 + \delta\lambda \qquad (35)$$

and the perturbation inflow is given by

$$\delta\lambda = \lambda_1 + \lambda_{1c} \, (r/R) \cos\psi + \lambda_{1s} \, (r/R) \sin\psi \tag{36}$$

The inflow variables λ_1, λ_{1c}, λ_{1s} which are functions of time are related to the perturbational thrust, roll and pitch moment coefficients, through the following relation

$$[M] \begin{Bmatrix} \overset{*}{\lambda}_1 \\ \overset{*}{\lambda}_{1c} \\ \overset{*}{\lambda}_{1s} \end{Bmatrix} + [L]^{-1} \begin{Bmatrix} \lambda_1 \\ \lambda_{1c} \\ \lambda_{1s} \end{Bmatrix} = \begin{Bmatrix} C_T \\ -C_{MY} \\ C_{MX} \end{Bmatrix}_{P.A.} \tag{37}$$

Where P.A. stands for perturbational aerodynamics. The elements of [L] can be determined either theoretically or experimentally.

For the present problem, where only the collective flap mode of the rotor is considered, the inflow variables λ_{1c} and λ_{1s} are not required. Therefore, the inflow equation for the collective mode can be written as

$$M_1 \overset{*}{\lambda}_1 + L_1 \lambda_1 = (C_T)_{P.A.} \tag{38}$$

Where M_1 represents the nondimensional apparent mass associated with the inflow variable λ_1. The value of M_1 is[16] $M_1 = 0.8488$, and the value of L_1 obtained from momentum theory[16] is $L_1 = 4\lambda_0$.

Equation (38) is complete only after identifying its right hand side. The expression for the perturbational thrust coefficient, can be obtained from blade element theory, and is given by

$$\rho \pi R^2 (\Omega R)^2 (C_T)_{P.A.} = \sum_{k=1}^{Q} \int_0^R \rho a b \Omega r (-r\Omega \overset{*}{\beta}_k - \lambda_1 \Omega R) dr$$

After integrating and applying the multiblade coordinate transformation, one has

$$(C_T)_{P.A.} = \frac{\sigma a}{2} \left[-\frac{\overset{*}{\beta}_m}{3} - \frac{\lambda_1}{2} \right] \tag{39}$$

Combining Eqs. (38) and (39) an equation for the inflow variable λ_1 is obtained. The equation for the collective flap mode is obtained by equating the inertia and the aerodynamic moments at the root. The equations for the collective flap mode and the inflow variable λ_1 are

$$\ddot{\beta}_m + \beta_m + \frac{\gamma}{2}\left[\frac{\dot{\beta}_m}{4} + \frac{\lambda_1}{3}\right] = 0 \tag{40}$$

$$M_1 \dot{\lambda}_1 + 4\,\lambda_0\,\lambda_1 = \frac{\sigma a}{2}\left[-\frac{\dot{\beta}_m}{3} - \frac{\lambda_1}{2}\right] \tag{41}$$

The various numerical quantities needed for evaluating Eqs. (40) and (41) are $M_1 = 0.8488$; $\lambda_0 = 0.05$; $\sigma = \frac{2Qb}{\pi R} = 0.061$, with $Q = 4$, $b/R = 0.024$; $a = 2\pi$ and $\gamma = 8.0$. Substituting these values in Eqs. (40) and (41) one obtains

$$\ddot{\beta}_m + \beta_m + \frac{\gamma}{2}\left[\frac{\dot{\beta}_m}{4} + \frac{\lambda_1}{3}\right] = 0 \tag{42}$$

$$0.8488\ \dot{\lambda}_1 + 0.2958\ \lambda_1 + 0.064\ \dot{\beta}_m = 0 \tag{43}$$

Computing the eigenvalues of the system represented by Eqs. (42) and (43) yields the following results. The eigenvalue $p_1 = -0.4015$ corresponds to the inflow mode associated with λ_1. The eigenvalue pair $p_{2,3} = -0.434 \pm i\ 0.871$ corresponds to the collective flap mode.

The results of these eigenvalue calculations are summarized for convenience in Table III. These results indicate that when using the finite state approximation to Loewy's lift deficiency function a 10% increase in flap damping is obtained, when compared to the results based on quasi-steady aerodynamics. The results based on the dynamic inflow model indicate a 13% reduction in flap damping when compared with quasi-steady aerodynamics.

The influence of dynamic inflow in rotor dynamic problems is frequently shown to be equivalent to a modification of the Lock number. Taking the Laplace transform of Eqs. (42) and (43) and substituting for λ_1 in terms of β_m yields

$$\left\{\tilde{s}^2 + 1 + \frac{\gamma}{8}\left[\frac{0.8488\ \tilde{s} + 0.2105}{0.8488\ \tilde{s} + 0.2958}\right]\tilde{s}\right\}\beta_m(\tilde{s}) = 0 \tag{44}$$

The underlined term in Eq. (44) also corresponds to a lift deficiency function. This term is similar to the low frequency approximation of Loewy's lift deficiency function, given by Eq. (34). Using Eq. (44) and denoting by C'_{DI} the lift deficiency function based on the dynamic inflow model, one obtains

$$C'_{DI}(\tilde{s}) = \frac{0.8488\ \tilde{s} + 0.2105}{0.8488\ \tilde{s} + 0.2958} \tag{45}$$

Substituting $\tilde{s} = i\omega/\Omega$ into $C_L'(\tilde{s})$ as defined by Eq. (34) and into Eq. (45) enables one to obtain a relation between the lift deficiency factor (or function) and the nondimensional frequency. The lift deficiency functions C_L', C_{DI}' together with the exact values of Loewy's lift deficiency function are shown in Fig. 7. It can be that the low frequency approximation to Loewy's lift deficiency function C_L' compares well with its exact values. On the other hand, the lift deficiency function based on the dynamic inflow model, Eq. (45) indicates different trends in both magnitude and phase. The magnitude of the exact value of Loewy's lift deficiency function starts from 1.0 and decreases as the frequency ω/Ω increases, whereas magnitude of the lift deficiency function C_{DI}', corresponding to dynamic inflow, starts from 0.7 and increases to 1.0 as ω/Ω increases. Also, the phase angle of the Loewy's lift deficiency function is always negative, however the phase angle obtained from C_{DI}' is always positive. A positive phase angle implies that the unsteady aerodynamic lift is leading the blade motion, and this results in the reduction of flap damping predicted by the dynamic inflow. This trend differs from the trend predicted by Loewy's unsteady aerodynamic theory in which the unsteady aerodynamic lift lags behind blade motion.

6. Conclusions

The most important conclusions obtained in this study are summarized below.

(1) In incompressible unsteady aerodynamic theories, the lift deficiency function plays the role of an aerodynamic transfer function relating the 3/4-chord downwash velocity to the lift on the airfoil. Therefore, the Bøde plot of the lift deficiency function can be used to obtain important information on the qualitative nature of the poles and zeros as well as their locations. Using this information, approximate finite state lift deficiency functions can be formulated for both the fixed wing case (i.e. Theodorsen's lift deficiency function) and the rotary wing case (i.e. Loewy's lift deficiency function).

(2) Indicial response functions were obtained using approximate aerodynamic transfer functions. It was found that the rotary wing indicial response functionhas an oscillatory nature, which causes the indicial response to overshoot its steady state value before reaching it. On the other hand, the fixed wing indicial response is nonoscillatory.

(3) The approximate, finite state, unsteady aerodynamic model obtained for Loewy's lift deficiency function, was applied to a simple rotor dynamic problem and used to determine the influence of unsteady aerodynamics on the flap damping of the rotor. It was found that unsteady aerodynamics increases the collective flap mode damping by 10% and increases the flap frequency by 6%, when compared to the results obtained with quasi-steady aerodynamics. The same rotor dynamic problem was also treated using dynamic inflow. The analysis with the dynamic inflow model indicated that the flap damping decreases by 13% compared to the results obtained with quasi-steady aerodynamics.

(4) An expression for a lift deficiency function based on dynamic inflow was derived and the magnitude and phase obtained from this lift deficiency function was found to differ from the values obtained from Loewy's lift deficiency function. Loewy's lift deficiency function predicts a negative phase angle (lag) between the lift on the airfoil and its motion, whereas the lift deficiency function based on dynamic inflow predicts a positive phase (lead) angle.

(5) The finite state unsteady aerodynamic model, obtained in this study has a number of potential important applications in rotary-wing aeroelasticity. In particular it would be useful in subcritical flutter testing as well as in the treatment of aero-servoelastic problems where one has coupling between an active control system and an aeroelastic system.

Acknowledgement

The authors would like to thank Mr. V. Ramanarayanan, California Institute of Technology, for the useful discussions regarding the modelling of transfer functions based on the Bode plot.

References

1. Theodorsen, T., "General Theory of Aerodynamic Instability and the Mechanism of Flutter", NACA Report 496, 1935.

2. Greenberg, J.M., "Airfoil in Sinusoidal Motion in Pulsating Stream", NACA TN 1326, 1947.

3. Loewy, R.G., "A Two-Dimensional Approximation to Unsteady Aerodynamics of Rotary Wings", Journal of the Aeronautical Sciences, Vol. 24, No. 2, February 1957.

4. Shipman, K.W., and Wood, E.R., "A Two-Dimensional Theory for Rotor Blade Flutter in Forward Flight", Journal of Aircraft, Vol. 8, No. 12, December 1971.

5. Edwards, J.W., "Unsteady Aerodynamic Modelling and Active Aeroelastic Control", SUDAAR 504, Stanford University, February 1977.

6. Dinyavari, M.A.H., "Unsteady Aerodynamics in Time and Frequency Domains for Finite-Time Arbitrary Motion of Rotary Wings in Hover and Forward Flight", Ph.D. Dissertation, Mechanical, Aerospace and Nuclear Engineering Department, University of California, Los Angeles, California, March 1985.

7. Vepa, R., "On the Use of Pade Approximants to Represent Unsteady Aerodynamic Loads for Arbitrary Small Motions of Wings", AIAA paper 76-17, AIAA 14th Aerospace Sciences Meeting, Washington, D.C., January 26-28, 1976.

8. Dowell, E.H., "A Simple Method for Converting Frequency Domain Aerodynamics to the Time Domain", NASA TM81844, 1980.

9. Dinyavari, M.A.H., and Friedmann, P.P., "Unsteady Aerodynamics in Time and Frequency Domains for Finite Time Arbitrary Motion of Rotary Wings in Hover and Forward Flight", AIAA Paper 84-0988, Proceedings of the AIAA/ASME/ASCE/AHS, 25th Structures, Structural Dynamics and Materials Conference, May 14-16, Palm Springs, California, pp. 266-282, 1984.

10. Ogata, K., Modern Control Engineering, Prentice-Hall, 1970.

11. Carpenter, P.J., and Fridovitch, B., "Effect of Rapid Blade-Pitch Increase on the Thrust and Induced-Velocity Response of a Full Scale Helicopter", NACA TN 3044, November 1953.

12. Bisplinghoff, R.L., Ashley, H. and Halfman, R.L., Aeroelasticity, Addison-Wesley, pp. 251-288, 1955.

13. Johnson, W., Helicopter Theory, Princeton University Press, 1980.

14. Venkatesan, C. and Friedmann, P., "Finite State Modelling of Unsteady Aerodynamics and Its Application to a Rotor Dynamic Problem", University of California at Los Angeles, School of Engineering and Applied Science Report, UCLA-ENG-85-10, March, 1985.

15. Dinyavari, M.A.H. and Friedmann, P.P., "Application of the Finite State Arbitrary Motion Aerodynamics to a Rotor Blade Aeroelastic Response and Stability in Hover and Forward Flight", AIAA Paper No. 85-0763-CP, Proceedings of the AIAA/ASME/ASCE/AHS 26th Structures, Structural Dynamics and Materials Conference, April 15-17, 1985, Orlando, Florida, pp. 522-535.

16. Peters, D.A., "Hingeless Rotor Frequency Response with Unsteady Inflow", NASA SP-352, 1974.

17. Friedmann, P.P., and Venkatesan, C., "Influence of Various Unsteady Aerodynamic Models on the Aeromechanical Stability of a Helicopter in Ground Resonance", Proceedings of the 2nd Decennial Specialists' Meeting on Rotorcraft Dynamics, Ames Research Center, Moffett Field, California, November 7-9, 1984.

Table I Coefficients of the Approximate Transfer Function, Eq. (8)

N(ik)		D(ik)	
a_1	1.118	b_1	0.868
a_2	3.458	b_2	3.336
a_3	3.187	b_3	2.403
a_4	4.714	b_4	4.406
a_5	3.609	b_5	2.629
a_6	3.268	b_6	2.970
a_7	2.084	b_7	1.458
a_8	1.237	b_8	1.096
a_9	0.656	b_9	0.437
a_{10}	0.255	b_{10}	0.220
a_{11}	0.112	b_{11}	0.701×10^{-1}
a_{12}	0.268×10^{-1}	b_{12}	0.226×10^{-1}
a_{13}	0.951×10^{-2}	b_{13}	0.557×10^{-2}
a_{14}	0.123×10^{-2}	b_{14}	0.102×10^{-2}
a_{15}	0.340×10^{-3}	b_{15}	0.184×10^{-3}
a_{16}	0.167×10^{-4}	b_{16}	0.134×10^{-4}
a_{17}	0.32×10^{-5}	b_{17}	0.16×10^{-5}

Table II Poles and Zeros of the Approximate Transfer Function, Eq. (8)

Poles Roots of D(ik)	Zeros Roots of N(ik)
-0.0200 ± i 0.1293	-0.0138 ± i 0.1254
-0.0276 ± i 0.2617	-0.0183 ± i 0.2574
-0.0295 ± i 0.3859	-0.0212 ± i 0.3847
-0.0357 ± i 0.5127	-0.0259 ± i 0.5085
-0.0382 ± i 0.6293	-0.0344 ± i 0.6509
-0.0489 ± i 0.7558	-0.0511 ± i 0.7351
-0.0581 ± i 0.8262	-0.0655 ± i 0.8459
-0.0487 ± i 0.9259	-0.0445 ± i 0.9153
-0.2549	-0.5691

Table III Eigenvalue for the Flapping Dynamics Problem (for γ=8.0)

Modes	Aerodynamic Model		
	Quasi-Steady Aerodynamics Eq. (31)	Finite State Loewy's Model Eqs. (29) & (32)	Dynamic Inflow Model Eqs. (42) & (43)
Collective Flap Mode	-0.5 ± i 0.866	-0.551 ± i 0.919	-0.434 ± i 0.871
Augmented State	---	-3.252	-0.4015

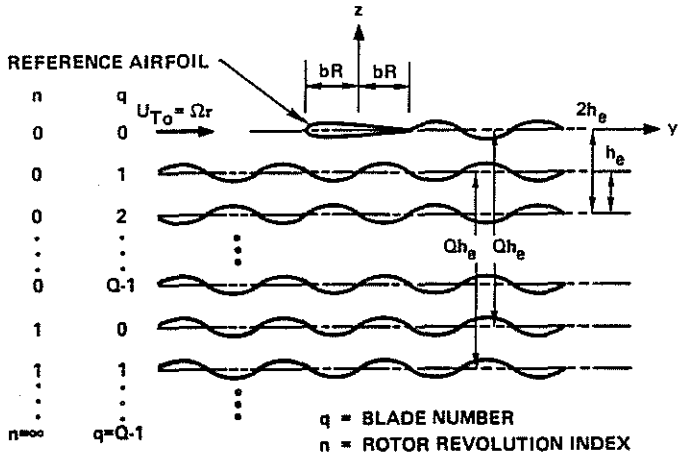

Fig. 1 Wake Structure for Loewy's Incompressible Aerodynamic Model

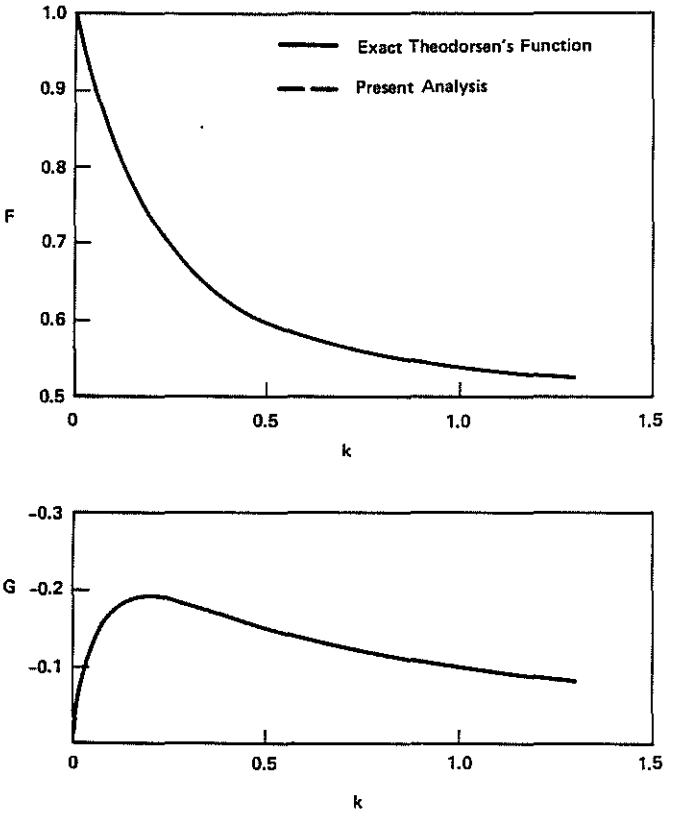

Fig. 2 Theodorsen's Lift Deficiency Function and Its Approximation Based on Three Poles

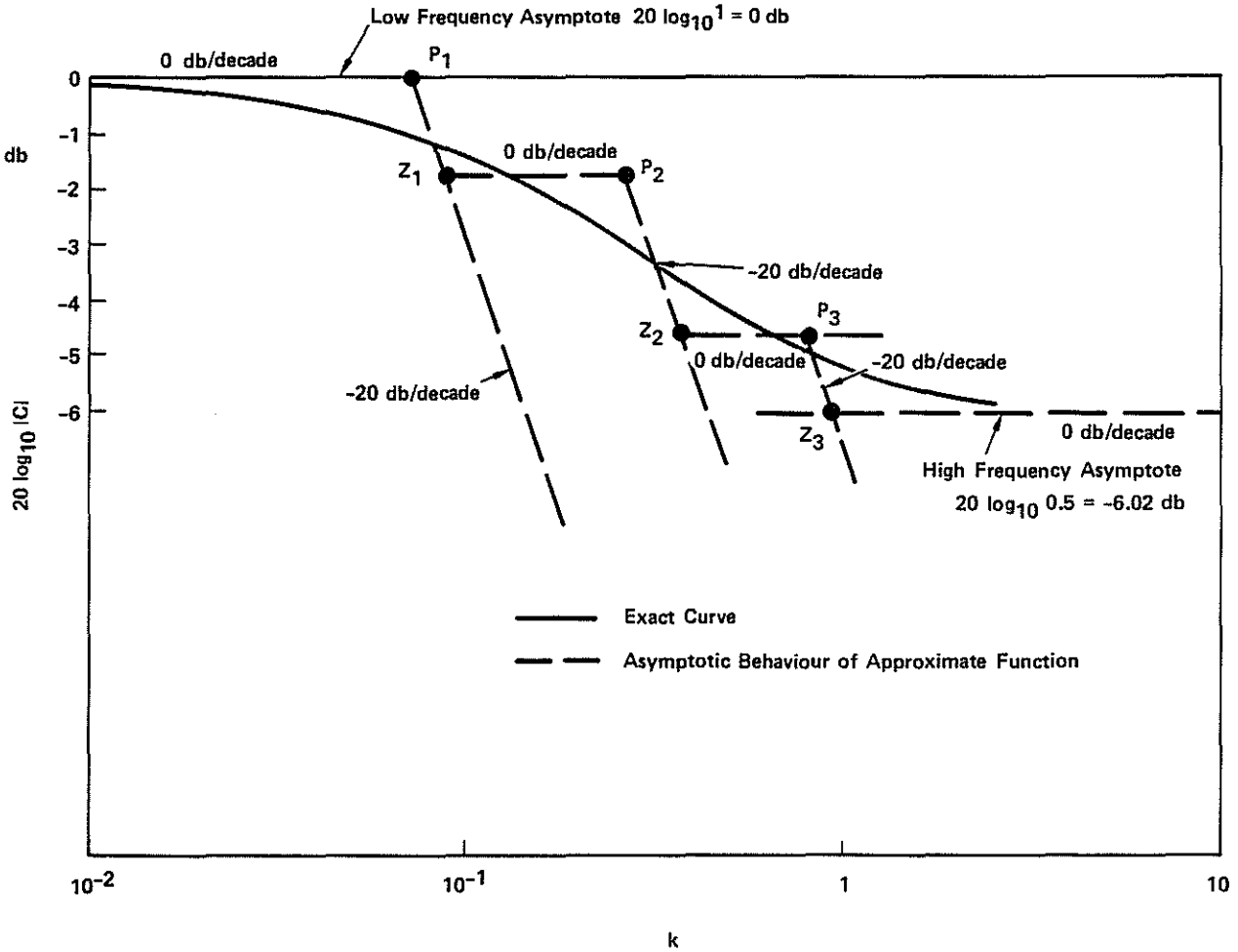

Fig. 3 Bode Plot of Theodorsen's Lift Deficiency Function, Exact Curve, and Approximation Using Three Poles

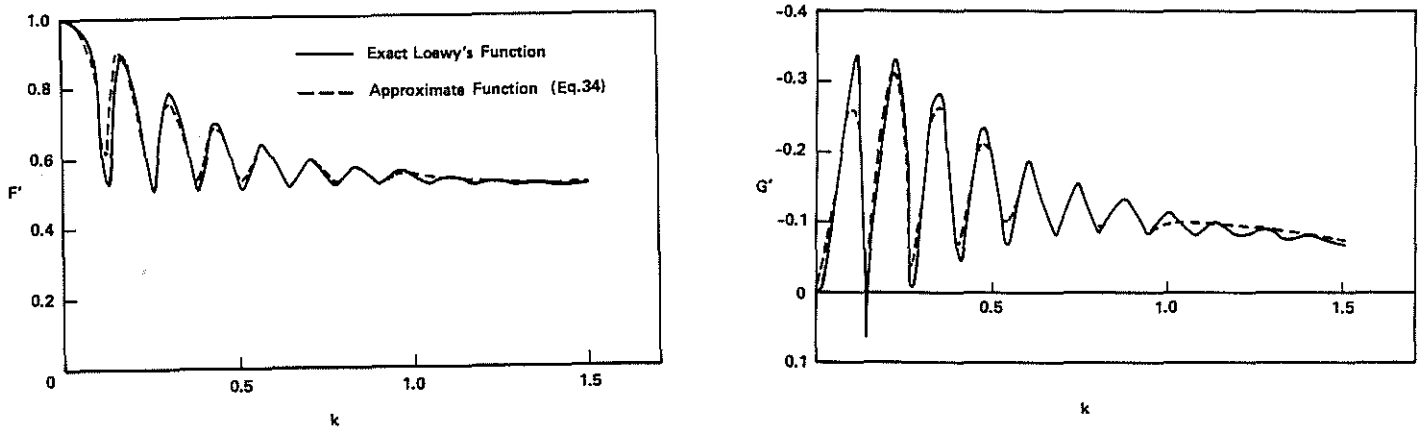

Fig. 4 Real and Imaginary Parts of Loewy's Lift Deficiency Function and Its Approximation

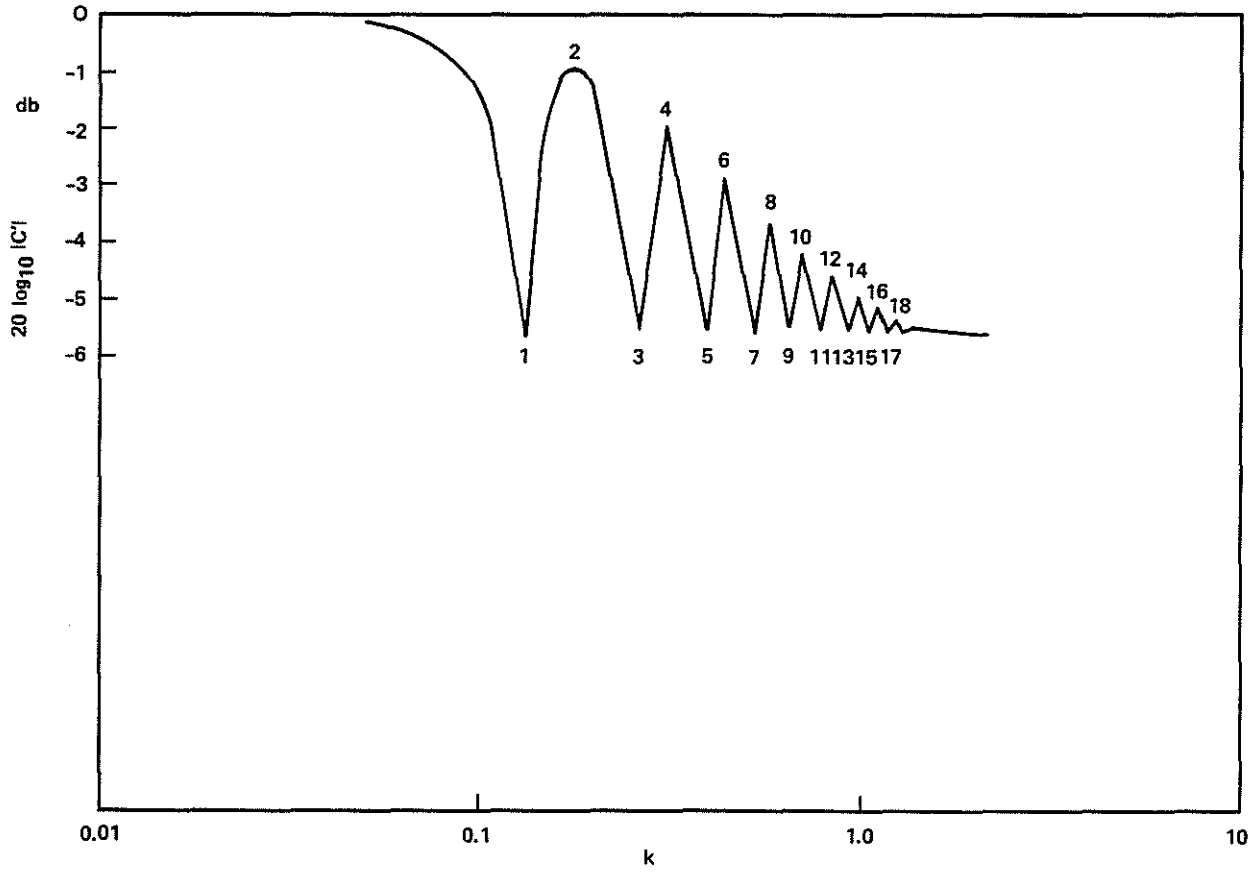

Fig. 5 Bode Plot of Loewy's Lift Deficiency Function

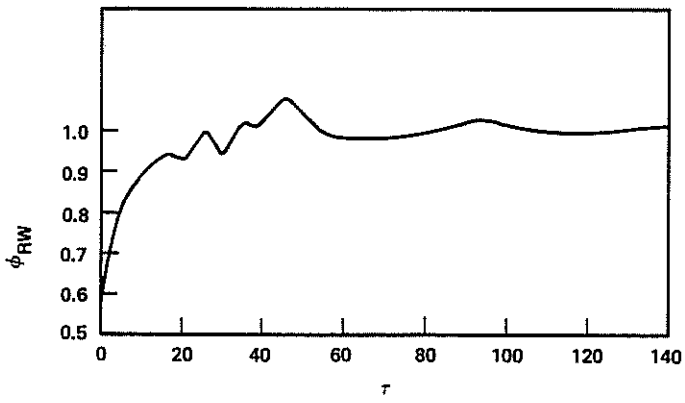

Fig. 6 Rotary Wing Indicial Response Function

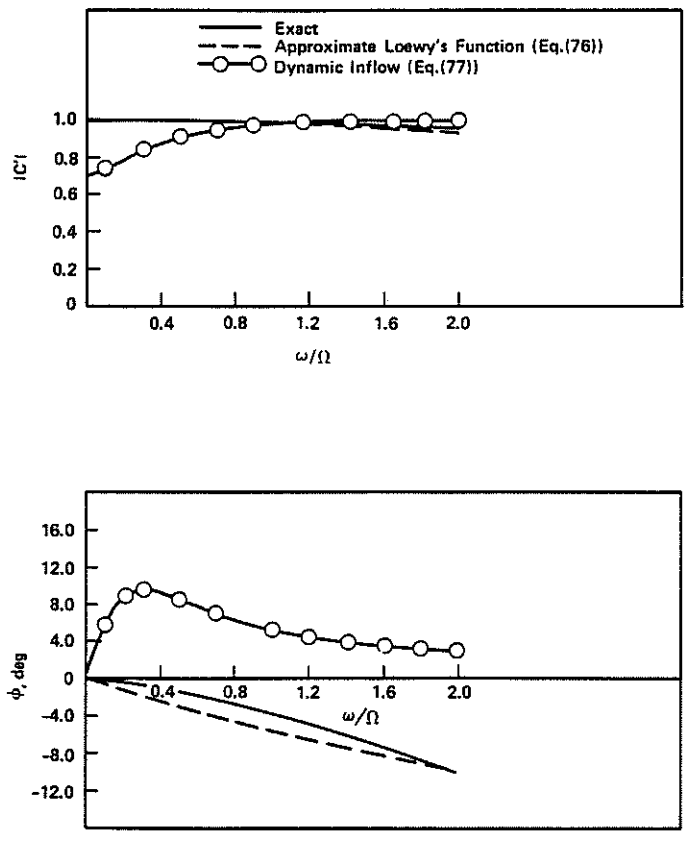

Fig. 7 Magnitude $|C'|$ and Phase ϕ of Various Lift Deficiency Functions